Supplementary Information for Interplay of spectral diffusion and phonon-broadening in single photo-emitters : the case of carbon nanotubes

A. Jeantet,[1] Y. Chassagneux,[1] T. Claude,[1] J. S. Lauret,[2] and C. Voisin[1]

[1] *Laboratoire Pierre Aigrain, École Normale Supérieure, CNRS, Université Pierre et Marie Curie, Université Paris Diderot, 24, rue Lhomond, F-75005 Paris, France*

[2] *Laboratoire Aimée Cotton, CNRS, Ecole Normale Supérieure de Cachan, Université Paris Sud, 91405 Orsay, France*

(Dated: November 9, 2017)

BLINKING SUPPRESSION

Encapsulating SWNTs in a layer of polymer is known to limit or altogether suppress time fluctuations such as bleaching and blinking[1,2]. In order to ascertain that no blinking distorts our analysis, the PL integrated intensity of the nanotubes displayed in fig. 2 and 3 of the main paper is plotted as a function of the time in fig. S1. Small fluctuations remain, with a standard deviation of 3% of the mean for the first nanotube and 5% for the second. We note that these fluctuations are slightly above the shot noise, but no on-off behavior is observable. If residual blinking remains, it is negligible at the PL integration timescales.

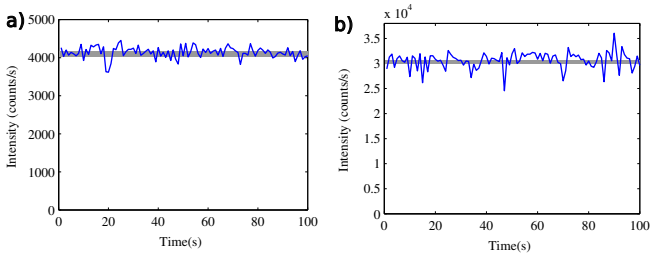

FIG. S1. (a) Spectrally integrated intensity of the nanotube displayed in fig. 1 of the main paper versus time (b) Integrated intensity of the nanotube displayed in fig. 2 of the main paper versus time. (a)(b) The shot noise is indicated by a gray zone

DERIVATIVE OF NANOTUBE 1

In the main paper, the method consisting in comparing the derivative of a spectrum $< \tilde{S} >$ to the mean difference between consecutive spectra is depicted in fig. 3. The same analysis was carried out for all the nanotubes of table I of the main paper. In particular, the data corresponding to the nanotube in fig. 2 of the main paper are shown in fig. S2.

ENERGY SHIFT

The PL of the nanotube investigated in fig. 3(d) of the main paper was monitored during 1000 s with an integration time of 100 ms. The energy of the ZPL $E(t)$

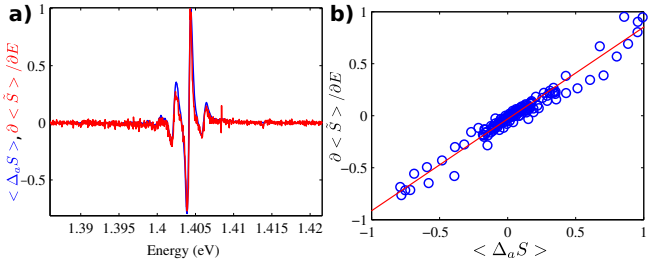

FIG. S2. (a) In red $\partial < \tilde{S} > /\partial E$. In blue the average of the difference between two consecutive spectra $< \Delta_a S >$. (b) The two quantities of figure (a) are plotted as a function of each other. The red line shows the linear behavior.

is plotted versus time in fig. S3(a). The histogram of the position is given in fig. S3(d). The distribution of positions is not Gaussian but remains confined to about 1 meV on each side of the mean position. Besides, one can observed spectral jumps at different timescales. The autocorrelation of $< |\delta E| >$ is given in fig. S3(c) and shows a decrease with characteristic time of a 100 s. The Fourier Transform of $< |\delta E| >$ (obtained using Matlab FFT function) is displayed in fig. S3(c).

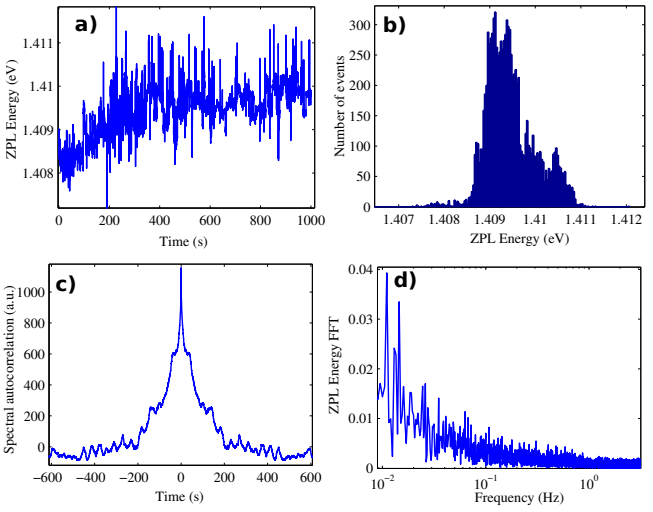

FIG. S3. (a) Evolution of the ZPL energy along time $E(t)$ expressed in eV. (b) Histogram of $E(t)$. (c) Autocorrelation of $\Delta E(t)$. (d) Fast Fourier transform of $\Delta E(t)$

Furthermore, an analysis of the evolution of $< |\delta E| >$

with the pump power was carried out. The mean energy shift $< |\delta E| >$ was extracted for the data shown in fig. 4(b) of the main paper. As visible in fig. S5(a) this energy shift is weakly sensitive to the input power over the two orders of magnitude explored here. However, recent experiments suggest that a sharper reduction of the input intensity may lead to a decrease of the photo-induced spectral diffusion and thus to a reduction of ZPL spectral width[3].

KOLMOGOROV-SMIRNOV TEST

The Kolmogorov-Smirnov test is a test without input parameters which aims to compare two distributions. For example, in fig. S4(a), a Lorentzian spectrum $S_1(x)$ with an intensity of 2 and a FWHM of 0.5 is plotted along with a Gaussian spectrum $S_2(x)$ with the same intensity and a FWHM of 2.35. The cumulative distribution function $F_{1,2}$ of these two spectra are given by

$$F_{1,2}(y) = \int I_y(S_{1,2}(x))dx \tag{1}$$

where

$$I_y(z) = \begin{cases} 0 & z > y \\ 1 & z < y \end{cases} \tag{2}$$

As shown in fig. S4(b), the KS test value is the maximum distance between these two cumulative distribution functions:

$$KS(S_1, S_2) = \max(|F_1 - F_2|) \tag{3}$$

This test is insensitive to a shift in abscissa. It returns 0 when two sets of data are identical (to a shift), and one if they are completely uncorrelated. Practically, the matlab function "kstest2" was used to analyze the experimental data. In order to compare a series of spectra to a series of reference, we compute an average KS value. For example, a series of N spectra $S_n(T_1, E)$ at temperature T_1 is compared to the reference series of N spectra $S_n(T_0, E)$ at temperature T_0). In order to increase the signal-to-noise ratio without lengthening exagerately the computation time, we compare each spectrum $S_n(T_1, E)$ to the first 10 spectra of the series $S_n(T_0, E)$ and average them out :

$$< KS >= \frac{1}{10N} \sum_{i=1}^{N} \sum_{j=1}^{10} KS(S_i(T_1, E), S_j(T_0, E)) \tag{4}$$

EFFECT OF THE EXPOSURE TIME

An appearant distortion of the spectra appears when comparing different integration times, as noted by Hofmann et al.[4]. The question arises whether this distortion

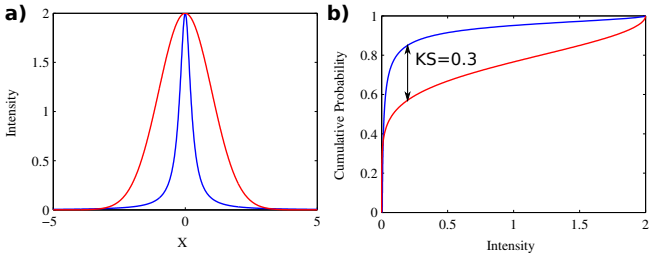

FIG. S4. (a) A Lorentzian spectrum with a FWHM of 0.5 (blue) and a Gaussian spectrum with a FWHM of 2.35 (red). (d) Cumulative distribution function of the two spectra in (a) (same color code). The maximum distance between the cumulative distribution functions is the KS value (black)

is simply a smoothing of the intrinsic profile (ZPL and wings) by random shifts of the spectrum, or whether an inhomogeneous distribution of the spectral shifts eventually warps the line profile. In order to investigate the effect of the exposure time on the spectral profile, 10 000 acquisitions were recorded with integration times of a 100 ms and averaged over a sliding window with a binning time ranging from 100 ms (no average) to 100 s. The mean energy shift as a function of the time binning is displayed in fig. S5(b) and shows a moderate increase with the time binning. In fig. S5(c), the spectra are plotted for binning times of 100 ms, 1 s, 10 s and 100 s. On can observe that the spectral diffusion yields a broadening of the spectra and a slight distortion of the ZPL for the larger binnings. However the profile (ZPL+wings) always holds. In fig. S5(d) one can see that the FWHM of the spectra scales as the square root of the time binning, a power law characteristic of diffusive processes. The full spectral profile was investigated by means of a KS test as shown in fig. S5(e). On the one hand, the blue dots compare two series of spectra averaged over the same binning time and display a KS value below 0.1, irrespective of the binning time. On the other hand, the black dots compare a series of averaged spectra with a series of raw spectra and show KS value quickly increasing with the binning time. This reflects the distortion of the spectra brought by the combination of long exposure and slow spectral diffusion. This explains the phenomenon observed by Hofmann et al.[4] : the whole spectrum shifts rigidly, but an integration time of tens of seconds artificially brings more complex features due to the different energies positions occupied over time.

LONG RANGE INTENSITY AUTOCORRELATION

The light emitted by the carbon nanotube is filtered with a 500 mm spectrometer and shone on a Perkin-Helmer avalanche photodiode. The slits of the spectrometer are adjusted to let only the ZPL go through, while the phonon wings are cut. As a consequence, when the

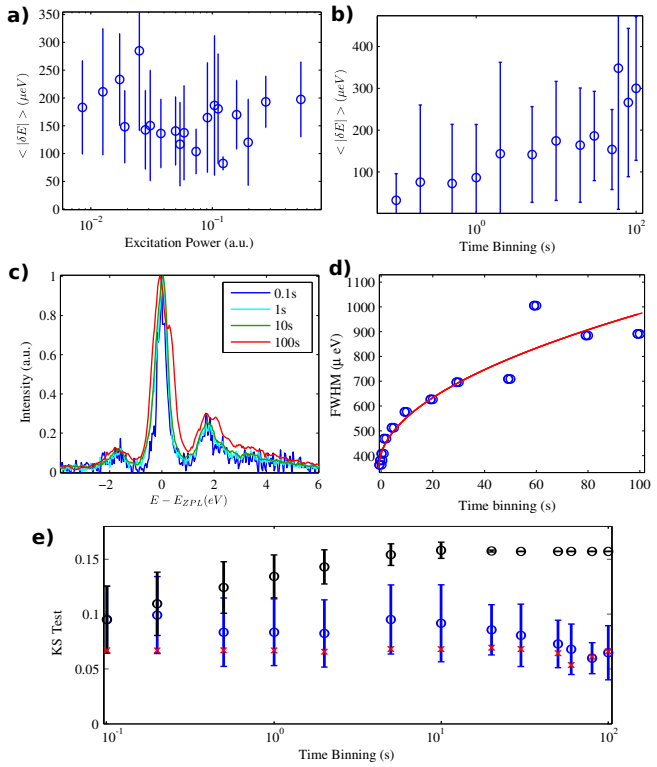

FIG. S5. a) Evolution of the mean energy shift $< |\delta E| >$ with the excitation power (semilog abscissa axis). (b) Evolution of the mean energy shift $< |\delta E| >$ with the time binning for time averaged spectra. (c) Evolution of the spectral profile as a function of the time binning (d) Evolution of the FWHM with time binning (e) KS test of a series of spectra at a given binning B in blue. KS test comparing spectra obtained from a binning B with spectra obtained without binning in black. Red crosses indicate the shot noise limit.

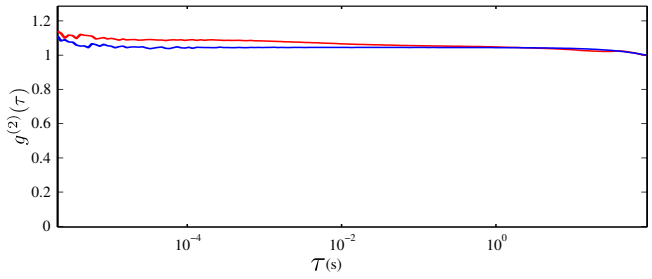

FIG. S6. Autocorrelation of the laser in blue and of the nanotube in red.

PL undergoes a spectral jump, the ZPL shifts out of the energy range selected by the slits, and the intensity $I(t)$ drops. We compute the long range intensity autocorrelation :

$$g^{(2)}(\tau) = \int \frac{I(t)I(t+\tau)}{< I(t)I(t+\tau) >} dt \qquad (5)$$

The nanotube PL autocorrelation is shown in fig. S6 along with the autocorrelation of the excitation laser; both are normalized on times over 10 s. The spectral diffusion observed down to 10 µs is of the same order than that measured on the second timescale.

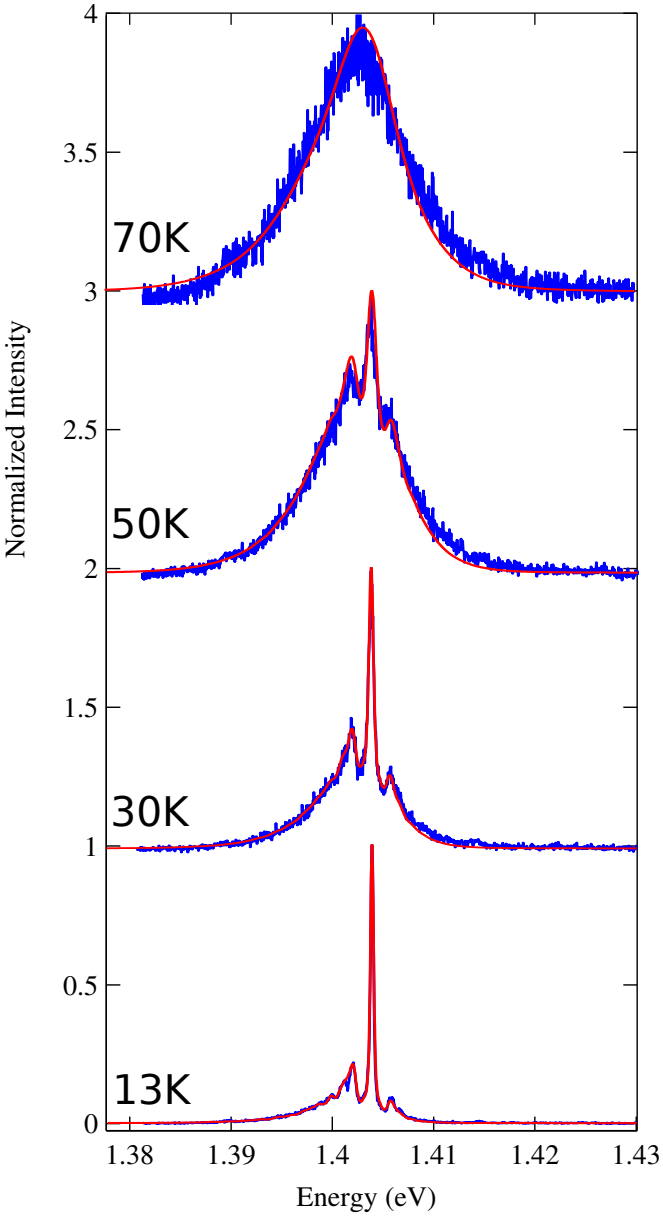

FIG. S7. Photoluminescence spectra of the same nanotube as in fig. 5 of the paper for temperatures of 13 K, 30 K, 50 K, 70 K. For each temperature, the fit obtained with the model of Vialla et al. is shown in red.

TEMPERATURE DEPENDENCE

In fig. 5 of the main paper, the temperature evolution of the PL of a single nanotube is shown and the dependence of the relative intensity between the red and blue wings is plotted for a given energy (1.8 ms of the ZPL energy). This shows in a simple way that the relative

intensities of the two wings are related to a Boltzmann factor. In order to go further, it is interesting to use the model developed by Vialla et al.[5]. It takes into account the full PL spectrum, the interaction between the localized exciton and the 1D phonons as well as the temperature. One can see in fig. S7 that this model fits well to our experimental data. The temperatures extracted from the fit are consistently higher of a few degrees than the measured one, as already noted by Vialla et al. Such a discrepancy can be explained if the temperature of the matrix is higher than the base plate temperature due to local heating by the pump.

[1] N. Ai, W. Walden-Newman, Q. Song, S. Kalliakos and S. Strauf, *ACS Nano*, 2011, **5**, 2664–2670.

[2] W. Walden-Newman, I. Sarpkaya and S. Strauf, *Nano Letters*, 2012, **12**, 1934–1941.

[3] Y. Luo, E. D. Ahmadi, K. Shayan, Y. Ma, K. S. Mistry, C. Zhang, J. Hone, J. L. Blackburn and S. Strauf, *arXiv preprint arXiv:1705.02034*, 2017.

[4] M. S. Hofmann, J. T. Glückert, J. Noé, C. Bourjau, R. Dehmel and A. Högele, *Nature nanotechnology*, 2013, **8**, 502–505.

[5] F. Vialla, Y. Chassagneux, R. Ferreira, C. Roquelet, C. Diederichs, G. Cassabois, P. Roussignol, J. S. Lauret and C. Voisin, *Phys. Rev. Lett.*, 2014, **113**, 057402.